

# REPORT DOCUMENTATION PAGE

Form Approved  
OMB No. 0704-0188

Public reporting burden for this collection of information is estimated to average 1 hour per response, including the time for reviewing instructions, searching existing data sources, gathering and maintaining the data needed, and completing and reviewing this collection of information. Send comments regarding this burden estimate or any other aspect of this collection of information, including suggestions for reducing this burden to Department of Defense, Washington Headquarters Services, Directorate for Information Operations and Reports (0704-0188), 1215 Jefferson Davis Highway, Suite 1204, Arlington, VA 22202-4302. Respondents should be aware that notwithstanding any other provision of law, no person shall be subject to any penalty for failing to comply with a collection of information if it does not display a currently valid OMB control number. PLEASE DO NOT RETURN YOUR FORM TO THE ABOVE ADDRESS.

1. REPORT DATE (DD-MM-YYYY) 12/16/2009	2. REPORT TYPE Final	3. DATES COVERED (From - To) 1/1/2007 - 11/30/2009		
4. TITLE AND SUBTITLE Ultrafast High Harmonic, Soft X-Ray Probing of Molecular Dynamics		5a. CONTRACT NUMBER		
		5b. GRANT NUMBER FA9550-07-1-0059		
		5c. PROGRAM ELEMENT NUMBER		
6. AUTHOR(S) Stephen R. Leone		5d. PROJECT NUMBER		
		5e. TASK NUMBER		
		5f. WORK UNIT NUMBER		
7. PERFORMING ORGANIZATION NAME(S) AND ADDRESS(ES)  Regents of the University of California University of California, Berkeley Sponsored Projects Office 2150 Shattuck Avenue, Suite 313 Berkeley, CA 94704-5940		8. PERFORMING ORGANIZATION REPORT NUMBER		
9. SPONSORING / MONITORING AGENCY NAME(S) AND ADDRESS(ES)  Dr. Michael Berman USAF, AFRL, AFOSR 875 N. Randolph Street Suite 325, Room 3112 Arlington, VA 22203		10. SPONSOR/MONITOR'S ACRONYM(S)		
		11. SPONSOR/MONITOR'S REPORT NUMBER(S)		
12. DISTRIBUTION / AVAILABILITY STATEMENT Approved for public release; distribution is unlimited.				
13. SUPPLEMENTARY NOTES				
14. ABSTRACT A three year program of experimental measurements in molecular dynamics was completed, using ultrafast soft x-rays produced by the method of pulsed laser high order harmonic generation and the vacuum ultraviolet synchrotron beamline at the Advanced Light Source. The experiments explored both small molecules and the intact ionic liquid molecules in the gaseous phase. Investigations probed the formation of intact ion pairs of aprotic ionic liquids in the vapor phase, the ultrafast fragmentation dynamics of ionic liquids, and the thermal decomposition of hypergolic ionic liquids, the latter in collaboration with Steven Chambreau and Ghanshyam (Gammy) Vaghjiani of Edwards Air Force Research Laboratory. Ionic liquids and cluster species have unique structures that involve the coupling of electron dynamics with vibrational, i.e. nuclear, motions. Thus the photofragmentation and decomposition pathways of ionic liquids are poised to undergo proton and electron transfers (charge transfer in excited electronic states) and reactive chemistry that are unlike most molecules when promoted to low energies of excitation. To understand this unique chemistry, these pathways were investigated by powerful methods to determine the novel internal reactive chemistry that will occur. Experiments were also performed on superexcited states of nitrogen. X-ray sources based on ultrafast lasers offer promise to complement synchrotron radiation as a convenient and more widely available means for chemical analysis, which will be of great interest to the Air Force and for the training of students. The goal of this research is to study ultrafast processes in molecular systems relevant to chemical and material properties of interest to the Air Force.				
15. SUBJECT TERMS Laser, X-Ray, Ionic Liquid				
16. SECURITY CLASSIFICATION OF:  a. REPORT Unclassified		17. LIMITATION OF ABSTRACT Unclassified	18. NUMBER OF PAGES 19	19a. NAME OF RESPONSIBLE PERSON Stephen R. Leone
b. ABSTRACT Unclassified		19b. TELEPHONE NUMBER (include area code) 510-643-5467		
c. THIS PAGE Unclassified				

## Final Report

### Ultrafast High Harmonic, Soft X-ray Laser Probing of Molecular Dynamics

Stephen R. Leone - Principal Investigator

## Introduction

With AFOSR support (FA9550-07-1-0059, entitled "Ultrafast High Harmonic, Soft X-ray Laser Probing of Molecular Dynamics"), the method of high order harmonic generation of ultrashort vacuum ultraviolet pulses was used to investigate molecular photodissociation, superexcited states, and ionic liquids. High order harmonics of a femtosecond Ti:sapphire laser are produced in the vacuum ultraviolet or soft x-ray spectral regions by intensely focusing the laser output into a rare gas jet.<sup>1</sup> By combining these outputs with visible and ultraviolet pump pulses in a pump-probe configuration, ultrafast photoelectron spectroscopic measurements are performed in the vacuum ultraviolet. The objectives of the proposed research are three fold: (A) to study ultrafast dynamics of ionic liquid vapor species photodecomposition, (B) to investigate thermal dissociation pathways of hypergolic ionic liquid vapors, and (C) to study small molecule dynamics by time-resolved soft X-ray spectroscopy. The approach is to produce ultrafast vacuum ultraviolet and soft x-rays through the process of high order harmonic generation and to couple these ultrashort pulses with visible or ultraviolet pulses for time-resolved dynamics investigations using mass spectrometry detection methods.

Earlier work used high order harmonic radiation and femtosecond soft x-ray pulses for several new experiments: time-resolved photoelectron spectroscopy of molecular fragmentation processes;<sup>2-5</sup> phase shaping of the harmonic pulses themselves;<sup>6</sup> the preparation and observation of Rydberg wave packets;<sup>7</sup> and imaging of time-resolved photoelectron angular distributions during Rydberg wave packet motion.<sup>8,9</sup> In addition, related experiments combined synchrotron radiation in the vacuum ultraviolet or soft x-ray regime with pulsed optical laser excitation for two-color<sup>10</sup> and high resolution core level spectroscopy.<sup>11</sup>

# Final Report

AFOSR Grant FA9550-07-1-0059

(Grant Period: 1 January 2007 – 30 November, 2009)

Recent developments in the generation of high-order harmonics<sup>12-16</sup> with femtosecond laser pulses in rare gases offer excellent opportunities for the experimental investigation of time-resolved valence- and core-level spectroscopy of dynamical processes in atoms and molecules. Until recently, these laser sources were primarily investigated by groups working on the harmonic generation process itself. Now the high harmonic process can be used to address a number of intriguing chemical and materials problems of interest. High harmonic sources can produce up to 1000 eV photon energies,<sup>15</sup> attosecond pulses,<sup>17-23</sup> and can generate photon fluxes with as high as  $\mu$ J energies per harmonic per pulse,<sup>24,25</sup> depending on wavelength. In work here, harmonics up to 100 eV photon energy are used; these wavelengths are also referred to as extreme ultraviolet (EUV and XUV).<sup>26</sup> The terminology "soft x-ray" is used here as a simplified descriptor for the high harmonic radiation, no matter what wavelength. This final report provides (A) brief highlights of the instrumentation developed in this laboratory for ultrafast soft x-ray probing of molecular dynamics and (B) results of recent investigations.

## A. Apparatus for Ultrafast Soft X-Rays

The apparatus constructed for ultrafast soft x-ray research is illustrated in Fig. 1.<sup>1</sup> It consists of a 1000 Hz Ti:sapphire laser that produces 2.5 mJ per pulse at 800 nm with pulses of 70 fs duration, a cell or jet of high density rare gas that is used for the harmonic generation source, a vacuum chamber to introduce gaseous samples, and a time-of-flight magnetic bottle photoelectron spectrometer or time-of-flight mass spectrometer. The apparatus incorporates frequency doubling and tripling of the Ti:sapphire fundamental pulses in nonlinear crystals to generate a separate pump (or probe) pulse, and the high harmonic pulses are used for the probe (or pump pulse). The timing is achieved by an optical delay line on the visible/ultraviolet pulse. A grazing incidence grating is used to select individual harmonics, for energy-selected probing in either photoelectron or mass spectrometry (ionization) experiments.

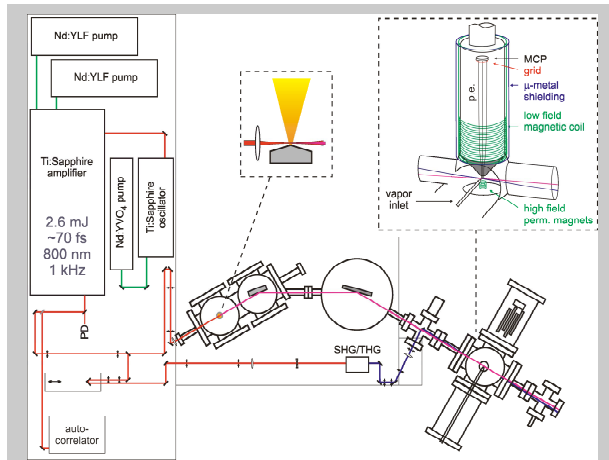


Figure 1. Apparatus for generating high order harmonics for photoelectron spectroscopy and mass spectroscopy using pump/probe time-resolved methods with soft x-ray harmonics.

For the process of high order harmonics in rare gases, the laser is focused to  $10^{14}$ - $10^{15}$  W cm $^{-2}$  in a high density of a rare gas ( $\approx 10^{18}$  cm $^{-3}$ ) in a pulsed jet or cell. Semiclassically, the mechanism involves driving an electron away from the ionic core of the rare gas and then, on the opposite cycle of the light, driving the electron back into the core, whereupon the harmonic light is generated by the recombination of the returning electron with the core.<sup>13</sup> The light is produced with good efficiency over a large number of odd harmonics up to a cutoff energy (Fig. 2). The odd harmonics are typical, resulting from symmetry in an isotropic medium. With this apparatus, harmonics of 800 nm light are produced up to the 65th ( $\approx 100$  eV) in Ne and excellent static photoelectron spectra are obtained with good signal-to-noise (100:1 in minutes).<sup>4</sup>

The magnetic bottle time-of-flight electron spectrometer,<sup>27-30</sup> based on a design of Neumark and co-workers,<sup>29</sup> incorporates a modification to shift the kinetic energies of the electrons from high to low values by a retarding grid system<sup>27,30</sup> to obtain high kinetic energy resolution even for high velocity electrons. The advantages of this system are the ability to collect a large solid angle of the emitted electrons and the elimination of stray electron signals by confining the zone of collection to a very small region around the high field magnets.

In some experiments, photoelectron spectra are acquired over a series of pump-probe time delays. For pump-probe experiments, often the signal-to-noise ratio must be on the order of 10000 or higher to obtain the desired differential changes in the photoelectron spectra. This is accomplished by subtracting signals of the pump only and the probe only from the pump+probe measurements. In other recent experiments on beams of ionic liquid molecules, the method of soft ionization of atomic and molecular fragments is employed. In that case the time-of-flight mass spectrometer is configured to detect ions, which is a technique newly introduced especially for the ionic liquid pump-probe experiments below.

Improvements to the apparatus include the mass spectroscopy detection of femtosecond pump-probe high harmonic experiments, better tools for alignment and detection of the temporal and spatial overlap of the high harmonics by using transitions in rare gases, phosphor detection of the harmonic beam location, implementation of "even" order high harmonics by the addition of 400 nm light to the 800 nm driver pulse, and beam oven sources for ionic liquids. With the close proximity of the Advanced Light Source to the femtosecond high harmonic laboratory, it

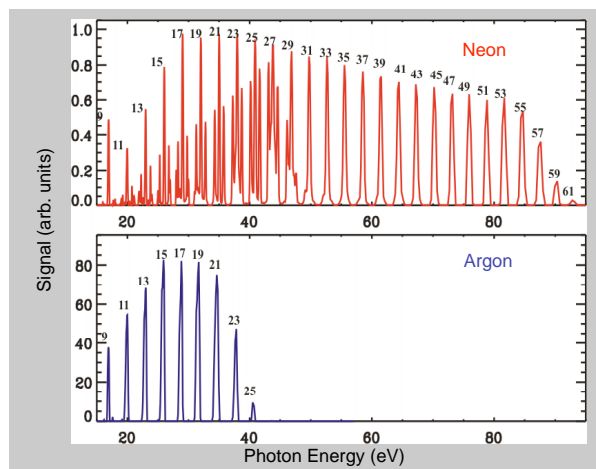


**Figure 2. High harmonics generated in neon and argon.** Note the lower energy cutoff in argon, the higher intensity from argon and the overlapping orders of the grating in the neon spectrum.

has also became possible to propose and obtain shifts to use the Chemical Dynamics Beamline for new experiments on ionic liquids. Together with Air Force Research Laboratory scientists Steven Chambreau and Ghanshyam Vaghjiani, new experiments have been performed to analyze the threshold photoionization energies and the fragmentation pathways of intact ionic liquid cation/anion pairs using the tunable synchrotron vacuum ultraviolet light.

## B. Recent Results of Ultrafast Soft X-Ray Photoelectron Probing

Several results of the experiments that were performed in the grant period are described below.

### 1. $^1\Pi_u$ dissociative state of $\text{Br}_2$

Single photon ionization with high order harmonics provides a general method to detect time-resolved processes, and it differs from multiphoton ionization detection because there are no complications due to resonant-enhanced absorption processes. Previous investigations of bromine molecules revealed a wave packet on a dissociative state for the first time in the photoelectron spectrum.<sup>3,5</sup> Here, femtosecond photoelectron spectroscopy is used to study new spectral shift information concerning the probing of the  $\text{C}^1\Pi_u$  dissociative state dynamics of  $\text{Br}_2$ .<sup>31</sup> Visible light at 402.5 nm is used to directly excite the dissociative state (pump) and 53.7 nm high harmonic radiation is used to detect (probe) the dynamics by ejecting photoelectrons. The magnetic bottle time-of-flight spectrometer is used to collect complete photoelectron spectra as a function of pump-probe delay. The depletion of the ground state bromine molecules is directly observed in the differential photoelectron spectra, as well as the rise of the  $\text{Br}^2\text{P}_{3/2}$  atom products, and, as noted above, transient features due to the wave packet on the dissociative state are observed. In addition, photoelectron peaks due to the  $\text{Br}_2^+(\text{X}^2\Pi_g)$ ,  $(\text{A}^2\Pi_u)$ , and  $(\text{B}^2\Sigma_g)$  ion states are observed (not shown here). Since the  $\text{Br}_2(\text{C}^1\Pi_u)$  state has the electron configuration  $2\sigma_g^2 1\pi_u^4 1\pi_g^3 2\sigma_u$  and the  $\text{Br}_2^+$  A state corresponds to the  $2\sigma_g^2 1\pi_u^3 1\pi_g^4$  configuration, the ionization to the  $\text{Br}_2^+(\text{A}^2\Pi_u)$  state requires a two electron transition (non-Koopman's theorem). Such transitions are typically weak, but there is extensive configurational mixing that occurs in diatomic halogen cations, resulting in structural anomalies in the  $\text{Br}_2^+(\text{A}^2\Pi_u)$  state.<sup>31,32</sup> Because the neutral  $\text{Br}_2$  ground state depletion and the rising neutral Br

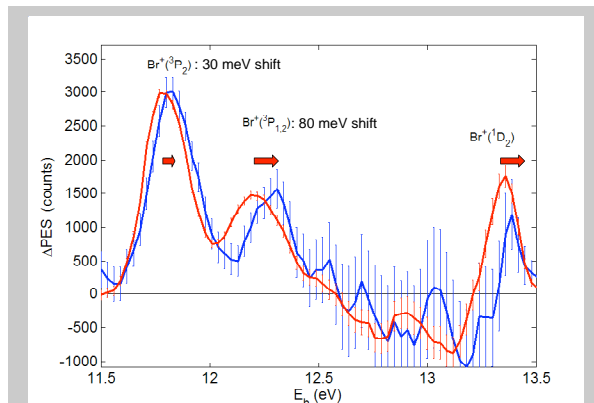


**Fig. 3** Photoionization spectra in the atomic Br region during the dissociative event, showing the shifts in energies from early to late time in the dissociation.

atomic peaks can both be observed in the same spectra, the relative photoionization cross sections for  $\text{Br}_2$  and Br atoms can be derived. Obtaining these partial cross sections, the ratio of  $\sigma[\text{Br}(^2\text{P}_{3/2}) \rightarrow \Sigma \text{Br}^+(^3\text{P}_{2,1,0})] : \sigma[\text{Br}_2(\text{X}^1\Sigma_g) \rightarrow \text{Br}_2^+(\text{X}^2\Pi_g)]$  is  $1.04 \pm 0.05$ . This result differs from early discharge flow measurements that are a factor of two higher.<sup>31</sup> Since both signals in the experiments are acquired simultaneously in the same spectrum, there is a high degree of confidence in the present results.

It was observed, in Fig. 3, that the photoelectron spectra of the atoms shift in time throughout the course of the dissociative event. In this figure, the data are binned from -200 fs to 200 fs in the red trace (essentially early times) and >200 fs in the blue trace (essentially late times). The peaks at the early times are shifted to higher binding energies. The shift of the  $\text{Br}^+ \text{D}_2$  is similar to 80 meV, however this peak is partly shifted outside the observed spectral region due to the applied deceleration field, so an exact shift is not labeled on the figure. The  $\text{Br}_2$  depletion peak is not shifted, excluding the possibility these shifts occur due to laser pulse chirp or some other artifacts. Variation of the power density of the 402.5 nm pulse also produces no shifts, indicating that the shifts are not due to ac Stark shifting effects. In Fig. 4 is shown the known potential curves in the region of interest. If the shift were due to the energy of the  $\text{C}^1\Pi_u$  state alone, the direction of the shifts would be opposite of the observations. The explanation for the shifts requires consideration of the upper state of the photoionization transition instead. Dissociative ionization states are known to contribute to the highly excited region where the 53.7 nm photons reach the ionization in  $\text{Br}_2$  from the  $\text{C}$  state,<sup>33</sup> as shown in Fig. 4. These dissociative ionization states do not contribute significantly to the shortest internuclear separations where the dissociation is initiated, however they contribute substantially to the longer internuclear separations as shown in the figure, causing the Br atoms to exhibit a shift in their photoelectron energy, not because of the gentle curvature of the  $\text{C}^1\Pi_u$  state (blue curve), but because of the greater curvature of the dissociative ionization states (red curve).

## 2. Superexcited States of $\text{N}_2$

Superexcited states<sup>34</sup> are neutral states of molecules that lie above the ionization continuum and can therefore undergo a number of nonradiative processes such as autoionization, dissociation into neutral excited states, or dissociative ionization. Such superexcited states are

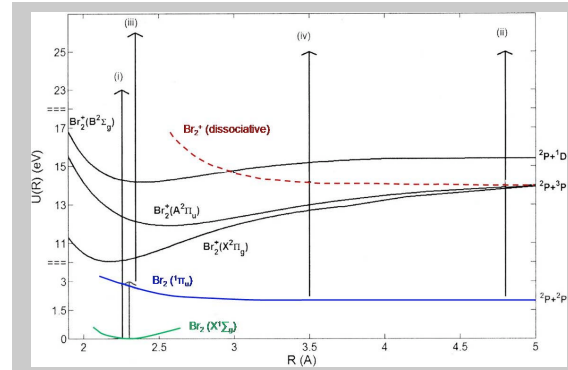


**Fig. 4** Potential curves for  $\text{Br}_2$  showing the dissociative ionization state that leads to shifts of the Br atoms at early times to higher binding energy. The red curve changes more rapidly to higher energies at short internuclear separations compared to the blue  $\text{C}^1\Pi_u$  dissociative state.

important in extreme environments such as ionized gases behind air-breathing scramjet engines<sup>35</sup> and re-entry vehicles,<sup>36</sup> having been caused by such processes as highly energetic electron collisions. Superexcited states also occur in the interstellar media and planetary ionospheres.<sup>37</sup> Accurate modeling of these environments requires detailed knowledge of the relaxation pathways and timescales of superexcited states.

Superexcited states can be categorized as singly excited valence or Rydberg states with sufficient rovibrational energy to autoionize and doubly electronically excited states above the ionization limit. The latter can undergo pure electronic autoionization on ultrafast timescales. While it is expected that these double electronically excited states will undergo rapid autoionization, it is not well-established whether the electronic doubly excited states also undergo favorably competing dissociation channels to produce electronically excited neutral atoms and molecular fragments or undergo rapid competing dissociative ionization pathways. In our recent work, doubly excited electronic levels of N<sub>2</sub> were produced directly by photoexcitation of N<sub>2</sub> molecules with the high harmonics, and fragment excited states of neutral N atom pathways were investigated on ultrafast timescales by a time-delayed 805 nm probe pulse for the first time (Fig. 5).<sup>38</sup>

Superexcited states of nitrogen (N<sub>2</sub>\*\*) may be accessed throughout the range of 21-38 eV. In the case of excitation of N<sub>2</sub> at 23.1 eV (53.7 nm), the nitrogen molecules have one electron excited to the n=4 or 5 Rydberg states, while simultaneously the core of the nitrogen ion is excited to the C<sup>2</sup>Σ<sub>u</sub><sup>+</sup> state (Fig. 5). It was previously observed that such states can predissociate, leading to emission from neutral excited N\*(3p <sup>4</sup>D<sup>0</sup>) and N\*(3p <sup>4</sup>P<sup>0</sup>) states.<sup>39,40</sup> In the experiments here, an 805 nm probe pulse can be used to interrogate the various N\* excited states by one and two photon ionization, as illustrated in the figure. In the results here, the power dependence of the probe pulse follows a one photon dependence (1.02±0.1), indicating that higher excited N\* states (3d or 4p) are most likely formed initially, which can be ionized with one photon, and these states may radiate in the near infrared to produce other observed emissions.

The energy of 23.1 eV was selected because it is below the 24.3 eV appearance energy of ground state N<sup>+</sup> ions, so that N<sup>+</sup> is only observed if the neutral N\* states are ionized by the 805

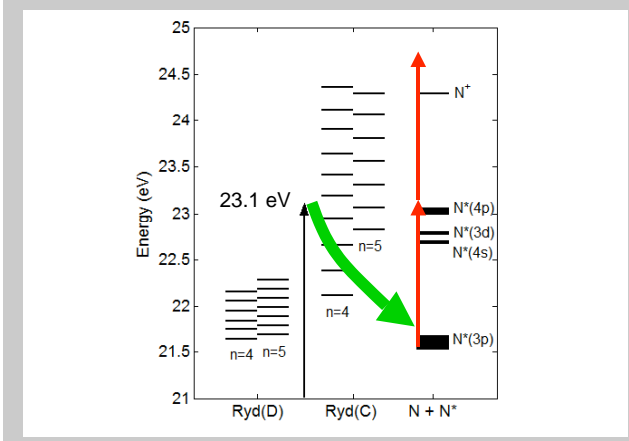
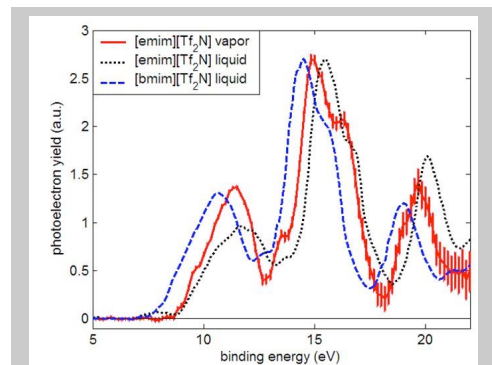


Fig. 5 Scheme for probing predissociative superexcited states of N<sub>2</sub> molecules by two photon ionization of N\*(3p) atoms or one photon ionization of N\*(3d or 4p) atoms.

nm probe pulse. The  $\text{N}_2^{**}$  can either autoionize to  $\text{N}_2^+$  +  $e^-$  or predissociate to  $\text{N} + \text{N}^*$  atoms. When a harmonic at 20 eV is selected, no  $\text{N}^+$  is observed with the 805 nm probe, indicating that there is no multiphoton dissociation of  $\text{N}_2^+$  ions by the 805 nm pulses. Via a series of measurements of the  $\text{N}^+$  signal versus pump-probe time delay, the appearance of  $\text{N}^+$  ions is detected with a risetime of less than 25 fs. The risetime is the sum of radiation, autoionization, and predissociation processes, with electronic autoionization likely to be the largest. The analysis required a deconvolution of the temporal dynamics of the high harmonic and laser pulses, which is measured using the 1s-3p resonant excitation of He atoms by a high harmonic followed by instantaneous probe ionization of the  $\text{He}^*$  atoms. The results, therefore, establish that the predissociation to  $\text{N} + \text{N}^*$  is competitive with autoionization of the doubly excited  $\text{N}_2^{**}(\text{C}^2\Sigma_u^+, n=4,5)$  states and the overall timescale for the sum of all processes is rapid.

### 3. Intact Ion Pairs in the Vaporization of Ionic Liquids

Ionic liquids are salts with melting points near or below room temperature. In recent years, ionic liquids composed of organic molecules, especially the dialkylimidazolium cations  $[\text{emim}]^+ = [\text{1-ethyl-3methylimidazolium}]$  cation, with counter anions such as  $\text{AuCl}_4^-$ ,  $\text{PF}_6^-$ ,  $\text{BF}_4^-$ ,  $[(\text{CF}_3\text{SO}_2)_2]\text{N}^- = [\text{bis}(\text{trifluoromethylsulfonyl})\text{imide}] = [\text{Tf}_2\text{N}]^-$ , etc., have found remarkable applications as solvents in synthesis and for multiphasic reactions because of their special solvating and electrochemical properties.<sup>41</sup> These new applications are now possible because of their wide liquid range, which encompasses room temperature for cation species such as  $[\text{emim}]$  and anion species such as  $[\text{Tf}_2\text{N}]$  (the explicit charges on these abbreviated subgroups will sometimes not be shown). Moreover, the direct extraction of ions from such ionic liquids by high voltages has been found to be an effective method for ion propulsion.<sup>42</sup> Recently, the synthesis of hypergolic ionic liquids (spontaneous ignition when combined with another reagent) has stimulated interest in novel ways to store chemical energy



**Fig. 6** Photoelectron spectra of  $[\text{emim}][\text{Tf}_2\text{N}]$  ionic liquid in the vapor phase (red line with error bars), compared to photoelectron spectra of the  $[\text{emim}][\text{Tf}_2\text{N}]$  liquid surface<sup>48</sup> (black dotted line) and  $[\text{bmim}][\text{Tf}_2\text{N}]$  liquid surface<sup>49</sup> (blue dashed line).

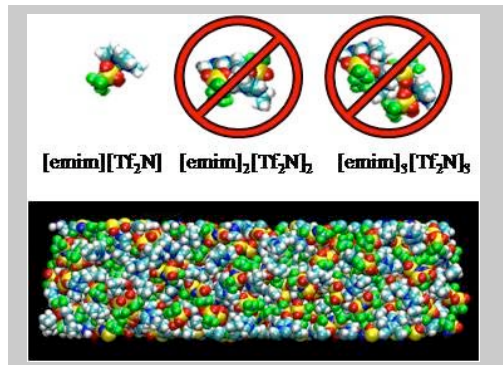


**Fig. 7** Structural simulation of  $[\text{emim}][\text{Tf}_2\text{N}]$  illustrating that neutral intact ion pairs, but not dimers or trimers, of the ionic liquid are formed in the vapor .

for propulsion in ionic liquids.<sup>43</sup> These low volatility and safe materials are of substantial importance to the Air Force for numerous reasons.

Calculations and measurements revealed much information about the fundamental properties of ionic liquids, but methods were lacking to investigate the intact ion pairs in the vapor phase until the demonstration that some ionic liquids could be volatilized without decomposition.<sup>44</sup> After this report, our group,<sup>45</sup> together with Edward Maginn, and several other groups,<sup>46,47</sup> rapidly established methods to vaporize ionic liquids to study their chemistry in the gas phase. In the case of the work in our laboratory,<sup>45</sup> an effusive molecular beam was constructed to produce beams of intact ionic liquids to measure photoelectron spectra and dissociative ionization mass spectra of the intact cation/anion pairs for the first time. The gas phase photoelectron spectra are compared to liquid phase (surface) photoelectron spectra<sup>48,49</sup> in Fig. 6.

The skinned beam produces intact molecules of ionic liquids, confirmed by subsequent <sup>1</sup>H and <sup>19</sup>F NMR of vaporized and collected samples deposited on a stainless steel plate. The photoelectron binding energy of gas phase [emim][Tf<sub>2</sub>N] is assessed to be 8.9±0.2 eV. Single photon ionization mass spectrometry reveals that the [emim]<sup>+</sup> cation is the dominant ion product, with a small amount of fragmentation (loss of ethyl) to form [methylimidazolium] cation = [mim]<sup>+</sup>. The mass spectral results suggest that the ionic liquid undergoes dissociative ionization with vacuum ultraviolet light and the 8.9 eV threshold is indicative of this dissociative ionization process.

There is good agreement between the photoelectron spectra of the liquid surfaces and the gas phase species. Results suggest that the gas phase species consist of intact cation/anion pairs, rather than clusters. This is confirmed by calculations of the group of Maginn.<sup>45,50,51</sup> The heat of vaporization of

[emim][Tf<sub>2</sub>N] is 146 kJ/mol, whereas the heats of vaporization to form the dimer [emim]<sub>2</sub>[Tf<sub>2</sub>N]<sub>2</sub> and trimer [emim]<sub>3</sub>[Tf<sub>2</sub>N]<sub>3</sub> are 187 kJ/mole and 227 kJ/mol, respectively. From the large differences in the energies, clustered species are not expected to occur significantly in the vapor. The ionic liquid vapor is mainly composed of isolated neutral intact [emim][Tf<sub>2</sub>N] cation/anion pairs, illustrated in Fig. 7.

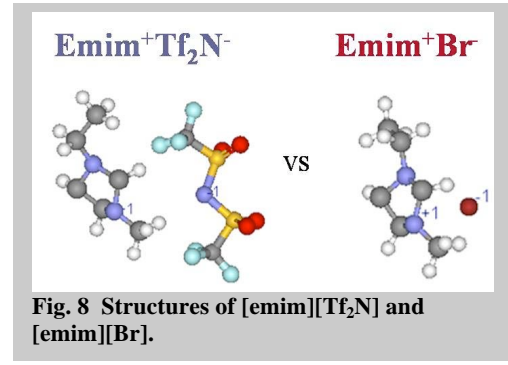


Fig. 8 Structures of [emim][Tf<sub>2</sub>N] and [emim][Br].

#### 4. Pump-Probe Dissociative Chemistry of Ionic Liquids

New ultrafast experiments were initiated to study the basic photo-dissociation dynamics of ionic liquids in the vapor phase. Two types of initial experiments have been performed. The first is to use multiphoton excitation (e.g. two-photon) at 400 nm to access a dissociative state of the ionic liquid vapor phase molecules, followed by multiphoton ionization of the fragments at 800 nm. These experiments are easy to perform and provide basic information, but did not readily obtain time information. The second was a more rigorous set of experiments using single photon ionization by the high harmonics as the probe. In both experiments, two conventional ionic liquid molecules are investigated,  $[\text{emim}][\text{Br}]$  and  $[\text{emim}][\text{Tf}_2\text{N}]$ ,<sup>52</sup> illustrated in Fig. 8. These were chosen because the  $[\text{Br}]$  anion is small and compact and is able to form a relatively tight binding to the  $[\text{emim}]$  cation, a binding that is potentially highly location-specific, whereas the  $[\text{Tf}_2\text{N}]$  anion is large and interacts with the  $[\text{emim}]$  cation over a very extended range. The idea is that there may be very specific fragmentation patterns that differ for different anions because of the interaction strength and location specificity of the anion. To illustrate some possible fragment pathways, a schematic diagram of a four-body dissociation of  $[\text{emim}][\text{Br}]$  is shown in Fig. 9. Whether these fragments will be neutrals or ions (e.g. imidazole neutral or imidazolium cation, bromine neutral atoms or bromide anion) and the specific patterns of the fragmentation, measured for the first time on isolated intact gas phase ionic liquids, are key goals of these experiments.

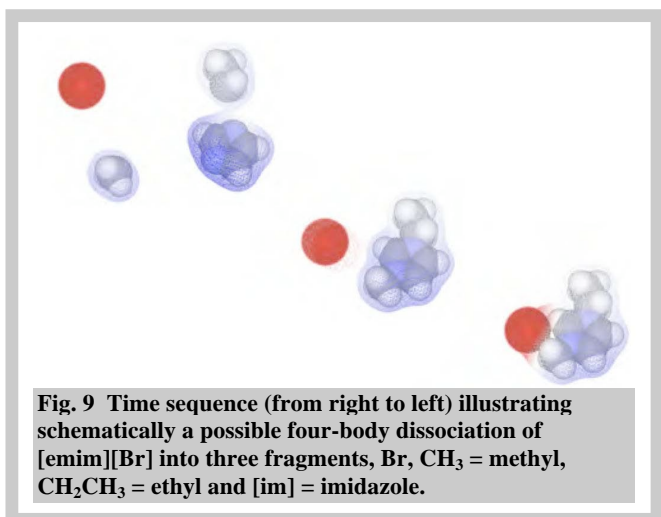


Fig. 9 Time sequence (from right to left) illustrating schematically a possible four-body dissociation of  $[\text{emim}][\text{Br}]$  into three fragments,  $\text{Br}$ ,  $\text{CH}_3$  = methyl,  $\text{CH}_2\text{CH}_3$  = ethyl and  $[\text{im}]$  = imidazole.

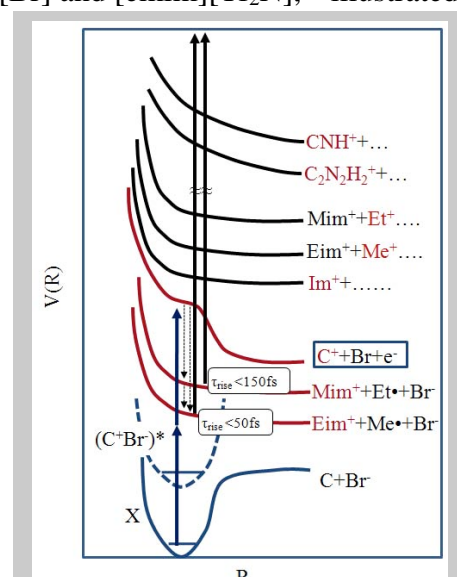
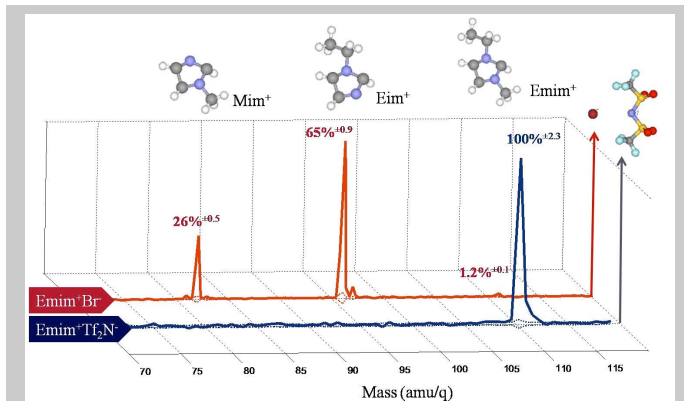


Fig. 10 Schematic potential curves of  $[\text{emim}][\text{Br}]$ , showing 400 nm excitation (blue) and single photon high harmonic ionization (black).

The imidazole ring  $\pi$  cloud can absorb two photons of visible or one photon of ultraviolet light via its electronic excitations,<sup>53-56</sup> and two photons of 400 nm light are already at an energy above that necessary to produce multiple dissociative pathways (Fig. 10); in the liquid phase the ion association enhances the visible absorption. In the gas phase the origin on the electronic



**Fig. 11** Mass spectra for photofragmentation of [emim][Br] and [emim][Tf<sub>2</sub>N] by 2 photons of 400 nm followed by 800 nm multiphoton ionization of the fragments.

shows one such pump-probe mass spectrum at  $\Delta t=0$  for the fragmentations of both [emim][Br] and [emim][Tf<sub>2</sub>N], demonstrating the dramatic differences in fragmentation patterns that occur. In all the experiments, the mass spectra are derived in a similar manner to previously described photoelectron spectra,<sup>31</sup> by subtraction of the signal of pump+probe minus the probe only and the pump only, thus eliminating processes due to the pump and probe alone. In the figure [eim] is ethyl imidazolium cation and [mim] is methyl imidazolium cation. The ionic liquid with the bromide [Br] anion has much richer fragmentation patterns compared to the larger [Tf<sub>2</sub>N] anion, possibly because there are many fewer degrees of freedom in [emim][Br], but also possibly because the [Br] anion interacts in a much more site-specific way with the [emim] cation and can undergo reactive chemistry. The [Br] may also have a greater charge interaction that alters the photon absorption probability in the ring. The photodissociation of [emim][Tf<sub>2</sub>N] shows only one positive ion mass peak, the [emim] cation, indicating a dissociation along the lines of the cation and anion pair, but the details of how the cation charge neutralization occurs in the

background is not so clear. Power dependence studies in our laboratory indicate that there are two photon excitations at 400 nm; an apparent one photon power dependence at 400 nm in [emim][Br] was observed and requires further investigations of the possible excited states or laser saturation effects. The first investigations take advantage of the two photon excitation of the ionic liquids at 400 nm, using time-delayed multiphoton ionization detection at 800 nm. Fig. 11

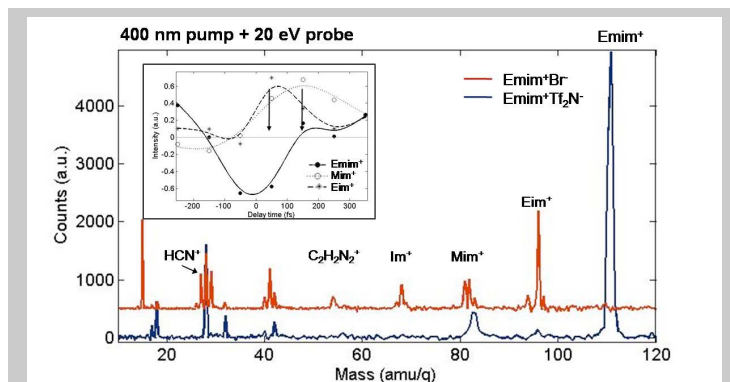


**Fig. 12** Differential pump-probe mass spectra at one time delay for two photon dissociation of [emim][Br] and [emim][Tf<sub>2</sub>N] and single photon ionization with the high harmonic probe. The inset shows some time behaviors.

dissociation must still be worked out. In contrast, the photofragmentation of [emim][Br] shows extensive loss of both methyl and ethyl fragments from the [emim] species, to form [mim] and [eim] neutral species, which then are detected by multiphoton ionization. Even though the potential curves in Fig. 10 show that the asymptotic limits of dissociative ionization states can be reached by two photons of 400 nm light, the particular fragments probed in these experiments by the time-delayed 800 nm multiphoton probe are the neutral species because of the systematic removal of pump only and probe only features by subtraction. Additional work will be needed to assess the direct dissociative ionization pathways. In Fig. 10, two timescales are shown, which are derived from high harmonic experiments below.

Multiphoton detection of fragmentation pathways is a method that is used extensively, yet the multiphoton ionization process itself can dissociate the very fragments we seek to detect. Thus experiments are performed using single photon ionization detection, taking advantage of the high harmonic source in our laboratory. Since the flux from the high harmonic probe is much less than the 800 nm multiphoton ionization probe directly from the pump laser, the high harmonic experiments require much more signal averaging. Nevertheless, first results have been obtained with a 20 eV probe, as illustrated in one example in Fig. 12.<sup>52</sup> One exciting result is that mass peaks are observed that suggest chemistry between the Br<sup>-</sup> and the imidazolium ring sites, indicating that intimate reaction chemistry can occur when the ionic liquid molecule is placed into electronically excited states. Mass peaks corresponding to species such as C<sub>2</sub>H<sub>2</sub>N<sub>2</sub><sup>+</sup>, C<sub>2</sub>H<sub>3</sub><sup>+</sup>, and HCN<sup>+</sup> are detected, in addition to [mim], [Hmim], [eim] and [emim]. The observation of HCN<sup>+</sup> detected from neutral HCN suggests a breakup of the imidazolium ring into several fragments, possibly by reaction of certain pieces of the ring and its substituents with the Br<sup>-</sup> when promoted to the electronically excited state. Second, time-resolved traces are also acquired with the single photon high harmonic probe, showing the rise of species such as [mim] and HCN. The results are preliminary, but highly encouraging, indicating that time-dependent dynamics with single photon detection can be exploited to study the photofragmentation dynamics of complex ionic molecules in the intact isolated vapor cation/anion pairs. Additional experiments are also required to determine what dissociative ionization pathways are occurring by the probe pulse itself, to vary the wavelength of the probe photon to minimize fragmentation pathways in the ionization detection, and to determine whether charge transfer processes occur in the dissociation.

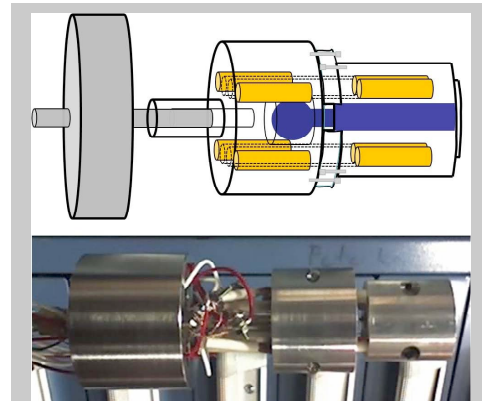


Fig. 13 Two stage oven for ionic liquid studies.

## 5. Hypergolic Ionic Liquids Decomposition

New experiments were initiated at the Advanced Light Source in collaboration with Steven Chambreau and Ghanshyam (Gammy) Vaghjiani of Edwards Air Force Research Laboratory to study the thermal decomposition of hypergolic ionic liquids. The goal of these experiments is to learn about the initial stages of decomposition to elucidate the mechanisms involved in the properties of hypergolicity.

Because the ionic liquids can decompose even during their vaporization process, we constructed a two-stage oven based on the principle of an arsenic cracker cell that has two independently heated regions, one to set the vapor pressure of the ionic liquid reservoir and the other to heat the vapor to cause thermal decomposition in a lower pressure regime as the vapor exits the oven (Fig. 13). This eliminates bimolecular collisions as a source of fragments from reactive chemistry. This oven was constructed in the shops prior to the second series of runs at the Advanced Light Source. Hypergolicity must produce a rapid heat release, by reaction, in a small volume. The understanding of thermal decomposition processes will therefore be important in understanding ignition also.

In a preliminary investigation with the synchrotron, non-hypergolic ionic liquids were investigated first to learn about their tunable-wavelength dissociative ionization thresholds. Shown in Fig. 14 are a series of results characterizing the ionization thresholds of three common ionic liquids, as labeled in the figure. Here the abbreviations [dmpim] = dimethyl-propylimidazolium cation and [Pf<sub>2</sub>N] = [bis(pentafluoroethylsulfonyl)imide] anion. The results show that higher resolution thresholds can be determined, and analysis is in progress to interpret the results of these threshold measurements.<sup>57</sup> In each case the formation of the parent cation [emim]<sup>+</sup> or [dmpim]<sup>+</sup> is measured as a function of tuning of the photon energy of the synchrotron. The results show that there are subtle shifts in the dissociative ionization energies as changes are made to the cation or anion species in each ionic liquid vapor. No parent cation counts are observed below these threshold energies, suggesting that dissociative ionization is the main mechanism accessed by the tunable vacuum ultraviolet photons, and not fragmentation to cation + anion species.

Studies were then pursued in two different runs at the Advanced Light source to investigate with Steven Chambreau the initial thermal decomposition pathways of a series of

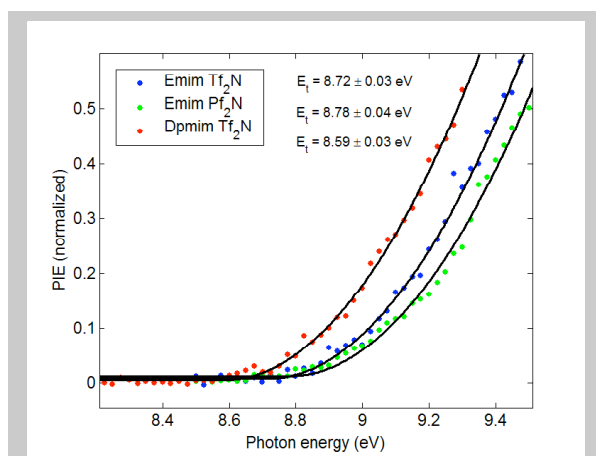
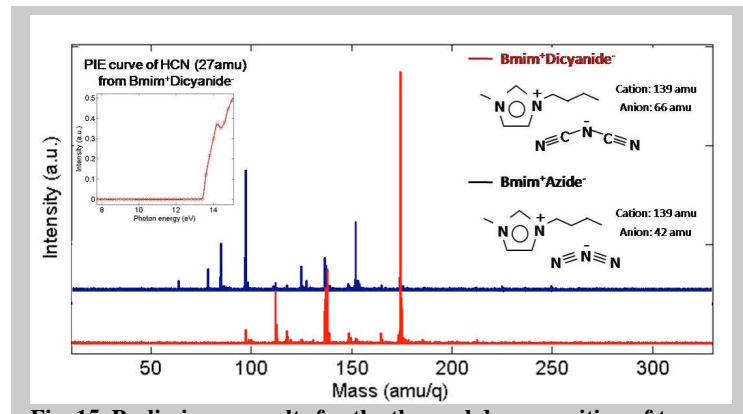


Fig. 14 Threshold energies for dissociative ionization of several ionic liquids, measured with the tunable synchrotron. PIE = photoionization efficiency.

hypergolic ionic liquids. The runs were performed with Leone group students and postdocs, who set up the apparatus and built the oven at the synchrotron and also helped to determine what experiments to pursue. The second run focused on the hypergolic ionic liquids based on the dicyanamide anions ( $\text{NCNCN}^-$ ),<sup>58,59</sup> which have been shown to react vigorously with fuming nitric acid to produce ignition; previous work on the azide anion ( $\text{N}_3^-$ ) species did not exhibit hypergolicity. An example of typical thermal decomposition mass spectra of the neutral species produced from the two different ionic liquids, dicyanamide (hypergolic) and azide (not hypergolic), interrogated by single photon ionization (8 eV) with the synchrotron is shown in Fig. 15. In this figure the synchrotron was set to a low photon energy, so that the neutral species are ionized near their thresholds, and the temperature of the oven was also set very low so that thermal decomposition and bimolecular collisions are both minimal. Thus the results at the lowest oven temperatures should establish a baseline for the initial decomposition pathways. Importantly, at higher probe photon energies,  $>13.4$  eV, which are sufficient to ionize HCN (see inset to Fig. 15), the HCN

neutral species at mass 27 is observed as a large signal in the hypergolic dicyanamide ionic liquid decomposition and is uniquely identified by its photoionization efficiency (PIE) curve of ion yield versus photon energy. Note that an HCN fragment was also observed in the laser photofragmentation of  $[\text{emim}][\text{Br}]$  discussed above, but this HCN is due to a different mechanism. The HCN in the dicyanamide ionic liquid may come from an H atom or proton transfer to the  $\text{NCNCN}^-$  anion, whereas in the pump-probe investigations of  $[\text{emim}][\text{Br}]$  the HCN most likely comes from the imidazolium ring. In future work the mass 150 and 178 species will be characterized.



**Fig. 15** Preliminary results for the thermal decomposition of two ionic liquids, measured with single photon ionization at the synchrotron. The observed photoionization efficiency curve for HCN is shown in the inset.

### Publications Sponsored by the project:

S. Gilb, V. Nestorov, S. R. Leone, J. C. Keske, L. Nugent-Glandorf, and E. R. Grant, "Kr ( $n=5$ -10, s, d, g) electronic wave packets: Electron time-of-flight resolution and the ac-Stark shift during wave-packet preparation," *Phys. Rev. A* **71**, 042709 (2005).

D. Strasser, T. Pfeifer, B. J. Hom, A. M. Müller, J. Plenge, and S. R. Leone, "Coherent interaction of femtosecond extreme-UV light with He atoms," *Phys. Rev. A* **73**, 021805 (2006).

S. Gilb, E. A. Torres, and S. R. Leone, "Mapping of time-dependent electron orbital alignment," *J. Phys. B: At. Mol. Opt. Phys.* **39**, 4231 (2006).

K. L. Knappenberger, Jr., S. Gilb, V. G. Stavros, E. W. Lerch, E. A. Torres, D. Strasser, L. Lau, and S. R. Leone, "Ultrafast wave packet, coherent control and dissociation dynamics," *Femtochemistry VII: Fundamental ultrafast processes in chemistry, physics, and biology*; Castleman, A. W., Jr., Kimble, M. L., Eds.; Elsevier: Amsterdam p. 14 (2006).

A. M. Müller, J. Plenge, S. R. Leone, S. E. Canton, B. S. Rude, and J. D. Bozek, "Core electron binding energy shifts of  $\text{AlBr}_3$  and  $\text{Al}_2\text{Br}_6$  vapor," *J. Electron Spectrosc. Related Phenom.* **154**, 32 (2006).

J. Plenge, C. Nicolas, A. G. Caster, M. Ahmed, and S. R. Leone, "Two-color visible/vacuum ultraviolet photoelectron imaging dynamics of  $\text{Br}_2$ ," *J. Chem. Phys.* **125**, 133315 (2006).

D. Strasser, F. Goulay, M. S. Kelkar, E. J. Maginn, and S. R. Leone, "Photoelectron spectrum of isolated ion-pairs in ionic liquid vapor," *J. Phys. Chem. A* **111**, 3191 (2007).

D. Strasser, F. Goulay, and S. R. Leone, "Transient photoelectron spectroscopy of the dissociative  $\text{Br}_2(^1\Pi_u)$  state," *J. Chem. Phys.* **127**, 84305 (2007).

D. Strasser, L. H. Haber, B. Doughty, and S. R. Leone, "Ultrafast predissociation of superexcited nitrogen molecules," *Molec. Phys.* **106**, 275 (2008).

S. D. Chambreau, G. L. Vaghjiani, A. To, C. Koh, D. Strasser, O. Kostko, and S. R. Leone, "Heats of vaporization of room temperature ionic liquids by tunable vacuum ultraviolet photoionization," *J. Phys. Chem. B* (submitted) (2009).

D. Strasser, F. Goulay, L. Belau, O. Kostko, C. Koh, S. D. Chambreau, G. Vaghjiani, M. Ahmed, and S. R. Leone, "Tunable wavelength soft photoionization of ionic liquid vapors," *J. Phys. Chem. A* (in press) (2009).

**Personnel:**

Daniel Strasser (postdoctoral associate, now assistant professor, The Hebrew University),  
Christine Koh (graduate student), Kyungwon Kwak (postdoctoral associate), Joshua Kretchmer  
(undergraduate student).

## References

1. L. Nugent-Glandorf, M. Scheer, D. A. Samuels, V. Bierbaum and S. R. Leone, "A laser-based instrument for the study of ultrafast chemical dynamics by soft x-ray-probe photoelectron spectroscopy," *Rev. Sci. Instrum.* **73**, 1875-1886 (2002).
2. L. Nugent-Glandorf, M. Scheer, M. Krishnamurthy, J.W. Odom and S. R. Leone, "Photoelectron spectroscopic determination of the energy bandwidths of high harmonics (7th-55th) produced by an ultrafast laser in neon," *Phys. Rev. A* **62**, 023812-1 (2000).
3. L. Nugent-Glandorf, M. Scheer, D. A. Samuels, A. M. Mulhisen, E. R. Grant, X. Yang, V. M. Bierbaum, and S. R. Leone, "Ultrafast time-resolved soft x-ray photoelectron spectroscopy of dissociating Br<sub>2</sub>," *Phys. Rev. Lett.* **87**, 193002 (2001).
4. L. Nugent-Glandorf, "Time resolved photoelectron spectroscopy with ultrafast soft x-ray light," Ph.D. Thesis, University of Colorado, Boulder (2001).
5. L. Nugent-Glandorf, M. Scheer, D. A. Samuels, V. M. Bierbaum and S. R. Leone, "Ultrafast photodissociation of Br<sub>2</sub>: Laser-generated high-harmonic soft x-ray probing of the transient photoelectron spectra and ionization cross sections," *J. Chem. Phys.* **117**, 6108 (2002).
6. D. Strasser, T. Pfeifer, B. J. Hom, A. M. Müller, J. Plenge, and S. R. Leone, "Coherent interaction of femtosecond extreme-UV light with He atoms," *Phys. Rev. A* **73**, 021805 (2006).
7. S. Gilb, V. Nestorov, S. R. Leone, J. C. Keske, L. Nugent-Glandorf, and E. R. Grant, "Kr (n=5-10, s, d, g) electronic wave packets: Electron time-of-flight resolution and the ac-Stark shift during wave-packet preparation," *Phys. Rev. A* **71**, 042709 (2005).
8. S. Gilb, E. A. Torres, and S. R. Leone, "Mapping of time-dependent electron orbital alignment," *J. Phys. B: At. Mol. Opt. Phys.* **39**, 4231 (2006).
9. K. L. Knappenberger, Jr., S. Gilb, V. G. Stavros, E. W. Lerch, E. A. Torres, D. Strasser, L. Lau, and S. R. Leone, "Ultrafast wave packet, coherent control and dissociation dynamics," *Femtochemistry VII: Fundamental ultrafast processes in chemistry, physics, and biology*; Castleman, A. W., Jr., Kimble, M. L., Eds.; Elsevier: Amsterdam p. 14 (2006).
10. J. Plenge, C. Nicolas, A. G. Caster, M. Ahmed, and S. R. Leone, "Two-color visible/vacuum ultraviolet photoelectron imaging dynamics of Br<sub>2</sub>," *J. Chem. Phys.* **125**, 133315 (2006).
11. A. M. Müller, J. Plenge, S. R. Leone, S. E. Canton, B. S. Rude, and J. D. Bozek, "Core electron binding energy shifts of AlBr<sub>3</sub> and Al<sub>2</sub>Br<sub>6</sub> vapor," *J. Electron Spectrosc. Related Phenom.* **154**, 32 (2006).
12. D. G. Lappas and A. L'Huillier, "Generation of attosecond XUV pulses in strong laser-atom interactions," *Phys. Rev. A* **58**, 4140 (1998).
13. K. J. Schafer and K. C. Kulander, "High-harmonic generation from Ultrafast Pump Lasers", *Phys. Rev. Lett.* **78**, 638 (1997).

14. I. P. Christov, M. M. Murnane, and H. C. Kapteyn, "High-harmonic generation of attosecond pulses in the 'single-cycle' regime," *Phys. Rev. Lett.* **78**, 1251 (1997).
15. C. Spielmann, C. Kan, N. H. Burnett, T. Brabec, M. Geissler, A. Scrinzi, M. Schnürer and F. Krausz, "Near-keV coherent X-ray generation with sub-10-fs lasers," *IEEE J. Q.E.* **4**, 249 (1998).
16. C. Spielmann, N. H. Burnett, S. Sartania, R. Koppitsch, M. Schnuerer, C. Kan, M. Lenzner, P. Wobrauschek, and F. Krausz, "Generation of coherent x-rays in the water window using 5-fs laser pulses," *Science* **278**, 661 (1997).
17. P. M. Paul, E. S. Toma, P. Breger, G. Mullot, F. Augé, Ph. Balcou, H. G. Muller, and P. Agostini, "Observation of a train of attosecond pulses from high harmonic generation," *Science* **292**, 1689 (2001).
18. M. Drescher, M. Hentschel, R. Kienberger, G. Tempea, C. Spielmann, G. A. Reider, P. B. Corkum, and F. Krausz, "X-ray pulses approaching the attosecond frontier," *Science* **291**, 1923 (2001).
19. M. Hentschel, R. Kienberger, Ch. Spielmann, G. A. Reider, N. Milosevic, T. Brabec, P. B. Corkum, U. Heinzmann, M. Drescher, and F. Krausz, "Attosecond metrology," *Nature* **414**, 509 (2001).
20. A. Scrinzi, M. Y. Ivanov, R. Kienberger, and D. M. Villeneuve, "Attosecond physics," *J. Phys. B: At. Mol. Opt. Phys.* **39**, R1-R37 (2006).
21. J. Levesque and P. B. Corkum, "Attosecond science and technology," *Can. J. Phys.* **84**, 1-18 (2006).
22. M. Drescher and F. Krausz, "Attosecond physics: facing the wave-particle duality," *J. Phys. B: At. Mol. Opt. Phys.* **38**, S727-S740 (2005).
23. T. Pfeifer, M. J. Abel, P. M. Nagel, A. Jullien, Z.-H. Loh, M. J. Bell, D. M. Neumark, and S. R. Leone, "Time-resolved spectroscopy of attosecond quantum dynamics," *Chem. Phys. Lett.* **463**, 11 (2008). (Frontiers Article)
23. I. P. Christov, H. C. Kapteyn, and M. M. Murnane, "Quasi-phase matching of high-harmonics and attosecond pulses in modulated waveguides," *Opt. Express* **7**, 362 (2000).
24. A. Paul, R. A. Bartels, R. Tobey, H. Green, S. Wieman, (I. P. Christov), M. M. Murnane, H. C. Kapteyn and S. Backus, "Quasi-phase-matched generation of coherent extreme-ultraviolet light," *Nature* **421**, 51 (2003).
25. K. Midorikawa, Y. Nabekawa, and A. Suda, "XUV multiphoton processes with intense high-order harmonics," *Prog. Quantum Electronics*, **32**, 43 (2008).
26. D. Attwood, "Soft x-rays and extreme ultraviolet radiation," Cambridge, Cambridge University Press (1999).
27. P. Kruit and R. H. Read, "Magnetic field paralliliser for 2p electron-spectrometer and electron-image magnifier," *J. Phys. E* **16**, 313 (1983).

28. O. Cheshnovsky, S. H. Yang, C. L. Pettiette, M. J. Craycraft, and R. E. Smalley, "Magnetic time-of-flight photoelectron spectrometer for mass-selected negative cluster ions," *Rev. Sci. Instrum.* **58**, 2131 (1987).
29. B. J. Greenblatt, M. T. Zanni, and D. M. Neumark, "Photodissociation dynamics of the  $I_2^-$  anion using femtosecond photoelectron spectroscopy," *Chem. Phys. Lett.* **258**, 523 (1996).
30. T. Tsuboi, E. Y. Xu, Y. K. Bae, and K. T. Gillen, "Magnetic bottle electron spectrometer using permanent magnets," *Rev. Sci. Instrum.* **59**, 1357 (1988).
31. D. Strasser, F. Goulay, and S. R. Leone, "Transient photoelectron spectroscopy of the dissociative  $Br_2(^1\Pi_u)$  state," *J. Chem. Phys.* **127**, 184305 (2007).
32. P. M. Boerrigter, M. A. Buijse, and J. G. Snijders, "Spin orbit interaction in the excited-states of the dihalogen ions  $F_2^+$ ,  $Cl_2^+$  and  $Br_2^+$ ," *Chem. Phys.* **111**, 47 (1987).
33. S. Leach, "Dissociative relaxation of  $I_2^+$ ,  $Br_2^+$ , and  $Cl_2^+$ ," *J. Phys. Chem.* **92**, 5373 (1988).
34. Y. Hatano, "Interaction of VUV photons with molecules - Spectroscopy and dynamics of molecular superexcited states," *J. Electron. Spectrosc. Rel. Phenomena* **119**, 107 (2001).
35. S. G. Chianese, K. K. Fisher, and M. M. Micci, presentation at the 37<sup>th</sup> AIAA/ASME/SAE/ASEE Joint Propulsion Conference and Exhibition, Salt Lake City, UT, p. 3937 (2001).
36. A. Bultel, B. G. Cheron, A. Bourdon, O. Motapon, and I. F. Schneider, "Collisional-radiative model in air for earth re-entry problems," *Phys. Plasmas* **13**, 43502 (2006).
37. E. Herbst, "Chemistry in the interstellar-medium," *Annu. Rev. Phys. Chem.* **46**, 27 (1995).
38. D. Strasser, L. H. Haber, B. Doughty, and S. R. Leone, "Ultrafast predissociation of superexcited nitrogen molecules," *Mol. Phys.* **106**, 275 (2008).
39. P. Erman, A. Karawajczyk, E. Rachlew-Kallne, J. R. I. Riu, M. Stankiewicz, K. Y. Franzen, and L. Veseth, "Neutral dissociation by non-Rydberg doubly excited states," *Phys. Rev. A* **60**, 426 (1999).
40. M. Ukai, K. Kameta, N. Kouchi, Y. Hatano, and K. Tanaka, "Neutral decay of double-holed doubly excited resonances of  $N_2$ ," *Phys. Rev. A* **46**, 7019 (1992).
41. P. Wasserscheid and T. Welton, eds., "Ionic liquids in synthesis," Weinheim, Wiley VCH (2004).
42. P. Lozano and M. Martínez-Sánchez, "On the dynamic response of externally wetted ionic liquid ion sources," *J. Phys. D: Appl. Phys.* **38**, 2371 (2005).
43. C. Bigler-Jones, R. Haiges, T. Schroer, and K. O. Christie, "Oxygen-balanced energetic ionic liquid," *Angew. Chemie* **118**, 5103 (2006).
44. M. J. Earle, J. M. S. S. Esperanca, M. A. Gilea, J. N. C. Lopes, L. P. N. Rebelo, J. W. Magee, K. R. Seddon, and J. A. Widgren, "The distillation and volatility of ionic liquids," *Nature* **439**, 831 (2006).

45. D. Strasser, F. Goulay, M. S. Kelkar, E. J. Maginn, and S. R. Leone, "Photoelectron spectrum of isolated ion-pairs in ionic liquid vapor," *J. Phys. Chem. A* **111**, 3191 (2007).

46. J. P. Armstrong, C. Hurst, R. G. Jones, P. Licence, K. R. J. Lovelock, C. J. Satterly, and I. J. Villar-Garcia, "Vapourisation of ionic liquids," *Phys. Chem. Chem. Phys.* **9**, 982 (2007).

47. J. P. Leal, J. M. S. S. Esperanca, M. E. Minas de Piedade, J. N. C. Lopes, L. P. N. Rebelo, and K. R. Seddon, "The nature of ionic liquids in the gas phase," *J. Phys. Chem. A* **111**, 6176 (2007).

48. O. Hofft, S. Bahr, M. Himmerlich, S. Krischok, J. A. Schaefer, and V. Kempter, "Electronic structure of the surface of the ionic liquid [EMIM][Tf<sub>2</sub>N] studied by metastable impact electron spectroscopy (MIES), UPS, and XPS," *Langmuir* **22**, 7120 (2006).

49. D. Yoshimura, T. Yokoyama, T. Nishi, H. Ishii, R. Ozawa, H. Hamaguchi, and K. Seki, "Electronic structure of ionic liquids at the surface studied by UV photoemission," *J. Electron Spectrosc. Relat. Phenom.* **144**, 319 (2005).

50. M. S. Kelkar and E. J. Maginn, "Calculating the enthalpy of vaporization of ionic liquid clusters," *J. Phys. Chem. B* **111**, 9424 (2008).

51. E. J. Maginn, "Atomistic simulation of the thermodynamics and transport properties of ionic liquids," *Acc. Chem. Res.* **40**, 1200 (2007).

52. C. Koh, D. Strasser, K. Kwak, and S. R. Leone, (in preparation).

53. A. Paul and A. Samanta, "Optical absorption and fluorescence studies on imidazolium ionic liquids comprising the bis(trifluoromethanesulphonyl)imide anion," *J. Chem. Sci.* **118**, 335 (2006).

54. E. Bernarducci, P. K. Bharadwaj, K. Krogh-Jespersen, J. A. Potenza, and H. J. Schugar, "Electronic structure of alkylated imidazoles and electronic spectra of tetrakis(imidazole)copper(II) complexes. Molecular structure of tetrakis(1,4,5-trimethylimidazole)copper(II) perchlorate," *J. Am. Chem. Soc.* **105**, 3860 (1983).

55. H. Chojnacki, "Electronic spectrum of  $\pi$ -electron delocalization of imidazole," *Theoret. Chim. Acta (Berl.)* **12**, 373 (1968).

56. R. Katoh, "Absorption spectra of imidazolium ionic liquids," *Chem. Lett.* **36**, 1256 (2007).

57. D. Strasser, F. Goulay, L. Belau, O. Kostko, C. Koh, Z.-H. Loh, M. Ahmed, S. Chambreau, and S. R. Leone, (in preparation).

58. S. Schneider, T. Hawkins, M. Rosander, G. Vaghjiani, S. Chambreau, and G. Drake, "Ionic liquids as hypergolic fuels," *Energy & Fuels*, **22**, 2871 (2008).

59. S. D. Chambreau, S. Schneider, M. Rosander, T. Hawkins, C. J. Gallegos, M. F. Pastewait, and G. L. Vaghjiani, "Fourier transform infrared studies in hypergolic ignition of ionic liquids," *J. Phys. Chem. A* **112**, 7816 (2008).